



Title	Chemical and medium-range orders in As ₂ S ₃ glass
Author(s)	Tanaka, Keiji
Citation	Physical Review B, 36(18), 9746-9752 https://doi.org/10.1103/PhysRevB.36.9746
Issue Date	1987-12-15
Doc URL	http://hdl.handle.net/2115/5730
Rights	Copyright © 1987 American Institute of Physics
Type	article
File Information	PRB36-18.pdf



[Instructions for use](#)

Chemical and medium-range orders in As_2S_3 glass

Keiji Tanaka

Department of Applied Physics, Faculty of Engineering, Hokkaido University, 060 Sapporo, Japan

(Received 18 June 1987)

Structures and optical-absorption edges of As_2S_3 glasses prepared by quenching at various temperatures have been studied. Raman scattering spectra show that the medium-range order decreases in the specimens rapidly quenched from temperatures higher than the glass-transition temperature, and that in the samples quenched from the vapor phase the homopolar-bond density is substantially increased. The medium-range order is recovered with annealing at the glass-transition temperature, and in contrast, for lessening the homopolar bonds and improving the chemical order, annealing at temperatures higher than the melting temperature is required. Increases in the structural disorders accompany red shifts of the optical-absorption edge and decreases in the slope of the Urbach tail.

I. INTRODUCTION

Amorphous materials are characterized by disorder or structural randomness, and atomic configurations of a material having a fixed chemical composition are different from sample to sample, depending on the preparation method and so forth.¹ The existence of a variety of amorphous structures is then tightly connected with another nature, i.e., the metastability. The material is in one of quasiequilibrium states having different internal energies. In a liquid, however, numerous disordered configurations can be regarded as a manifestation of thermal fluctuation. For a crystalline material, in contrast, we can in principle prepare a single crystal having a periodic structure, and its properties are uniquely determined under a combination of temperature and pressure.

The structural variations in amorphous semiconductors substantially modify the electronic properties. For instance, it is known that as-evaporated As_2S_3 films have wider optical energy gaps than those of annealed As_2S_3 films. DeNeufville² has demonstrated that the as-evaporated films are composed of molecular units intermixed in network structures, and that the annealed films are cross linked. Thus the electron wave functions in the as-evaporated films are assumed to be localized, and the interaction among electron orbitals belonging to different molecules is reduced. Bandwidths may, therefore, be smaller in as-deposited films, contributing to the blue-shifted absorption edges. In contrast, for amorphous GeSe_2 it has been shown that the optical-absorption edges of evaporated films are shifted to lower energies than those of melt-quenched glasses.³ A number of dangling and homopolar bonds in the film appear to be responsible for the red-shifted absorption edges.

For glassy materials, the diversity of properties may be reduced when the preparation method is restricted to melt quenching; however, the properties are still influenced by several parameters characterizing the quenching process. A well-known example is the fact

that the glass-transition temperature becomes higher with increasing quenching rate.¹ The relations between various properties and structures depending on preparation procedures, however, have not been fully studied so far.

In order to elucidate the correlation between structures and properties of amorphous semiconductors, we examine systematically the preparation dependence for As_2S_3 glass. The main reasons why this material was selected are that the energy gap of about 2.4 eV is pertinent to optical measurements and that the material hardly crystallizes thus permitting a wide range of preparation conditions.

In contrast to crystalline structures, atomic configurations of amorphous materials are not known explicitly, and therefore arguments on the properties may necessarily be weak, being constructed on speculative ideas. For obtaining insight as clear as possible, we will try to interpret the electronic and structural results in a coherent fashion, at least in a qualitative sense. In Sec. II experimental details are described. Section III provides results and discussion for properties of As_2S_3 glasses. Finally, we summarize arguments in Sec. IV. A preliminary result of the present work was published previously.⁴

II. EXPERIMENTS

As_2S_3 glasses were prepared as follows. A bulk ingot was synthesized in an evacuated ampoule by having elements of 99.9999% purity react at 800°C in a rocking furnace with subsequent quenching. The ingot was crushed, and chunks of 1 g were again vacuum sealed in quartz ampoules. The materials were heated in the furnace, stored for 10 h at various temperatures denoted as T_q , and then quenched into water or cooled down to room temperature in the furnace. Cooling rates of these two processes were estimated to be 10 and 10^{-2} K/sec. On the basis of previous results for quenching experiments,⁵ it could be assumed that the fast and slow cool-

ing rates are appropriate, respectively, to freeze high-temperature states and to produce stabilized glasses. It could also be assumed that the composition variation among the samples was small because of the above-mentioned procedure, and x-ray microprobe analyses indeed revealed that the variation was smaller than ± 1 at. %, the resolution being limited by the analyzing procedure.

The samples were annealed at a temperature denoted as T_a for 1 h. When $T_a \leq T_g$ (the glass-transition temperature), the annealing treatment was performed in a flowing Ar ambient. In contrast, when $T_a \geq T_g$ the glassy samples were annealed in vacuum-sealed quartz ampoules. For both treatments, specimens were slowly cooled to room temperature after being stored at T_a .

The bulk glasses were polished into parallel-sided wafers of thickness of 10–300 μm for optical transmittance measurements. The optical absorption coefficient α around the absorption edges was evaluated from the transmittance T by using an equation

$$\alpha = (1/d) \ln[(1-R)^2/T], \quad (1)$$

where d is the sample thickness and R is the reflectivity at sample surfaces. R was calculated using the Fresnel formula from the refractive index n given by Rodney *et al.*⁶ for glassy As_2S_3 . It is known that the magnitude of the refractive index depends on preparation procedures, e.g., at $\lambda = 6328 \text{ \AA}$, $n = 2.45$ for as-evaporated As_2S_3 films⁷ and $n = 2.61$ for Rodney's bulk glasses.⁶ The difference is 0.16, and the influence on α is less than 100 cm^{-1} . Taking gross structural differences between as-deposited films and bulk glasses into account,² it can be assumed that the variation of refractive indices among melt-quenched As_2S_3 samples is substantially smaller.⁸ Accordingly, errors introduced from neglecting slight modification of n may not be essential in the present discussion.

Raman scattering spectra were excited by an unfocused beam from a 15-mW He-Ne laser, and scattered light at a right angle was dispersed by a double monochromator and detected by a photon-counting apparatus. No polarization analyses were performed. Photoinduced changes² were not detected in the counting intervals of 1 h.⁹ Differential-scanning-calorimetry (DSC) thermograms were measured with a heating rate of 10 K/min ($= 0.2 \text{ K/sec}$) for samples of 5 mg contained in Al sample pans. X-ray diffraction experiments showed that all specimens exhibit no crystalline peaks. In addition, no discernible differences were observed among the x-ray patterns of As_2S_3 glasses having different T_q and the quenching rate.

III. RESULTS AND DISCUSSION

Figure 1 shows the DSC thermograms typical to slowly cooled and rapidly quenched samples from $T_q > 250^\circ\text{C}$. The inflection points in the thermograms, the temperatures of which correspond to T_g , are located at about 190°C , seemingly similar to each other. It is pointed out, however, that a hump is accompanied only with the glass-transition signal of the slowly cooled sample. According to Owen's argument¹ based on relaxa-

tional kinematics, existence of the hump indicates that T_g is lower than the inflection point of the DSC trace. The argument predicts that if the DSC heating rate were slower than the cooling rate of the sample preparation, the heat capacity would change at a lower temperature. (In the present experiment, the heating rate could not be arranged slower because of the small glass-transition signals.) Thus the hump is considered to be a signature indicating that the slowly cooled sample is more stabilized or nearer to the equilibrium state. A difference in DSC thermograms similar to Fig. 1 has been detected between as-evaporated and annealed As_2S_3 films.¹⁰

A. Optical-absorption edge

Figure 2 shows the optical-absorption edges of slowly cooled and rapidly quenched glasses from 650°C . We see that when $\alpha \approx 10^2 \text{ cm}^{-1}$ both samples exhibit the characteristics represented by

$$\alpha \propto \exp(\Gamma \hbar\omega), \quad (2)$$

where Γ may be called the Urbach parameter¹¹ and $\hbar\omega$ is the photon energy. There are, however, distinct differences between the two samples. The quenched glass shows a less steeper absorption tail located at a lower-energy side than that for the stabilized sample. The location and the steepness parameter may be good measures of the optical absorption edges, and hence we will evaluate the optical energy gap E_g defined as the photon energy where $\alpha = 1 \times 10^3 \text{ cm}^{-1}$. We also examine Γ calculated at $\alpha = 1 \times 10^2 \text{ cm}^{-1}$.

The dependence of E_g on T_q is shown in Fig. 3(a). Irrespective of T_q values, all slowly cooled samples exhibit a fixed E_g of $2.43 \pm 0.01 \text{ eV}$, implying a unique electronic property. In contrast, quenched samples reveal a peculiar variation. When $T_q \leq T_g$, E_g is the same as that of the stabilized sample, the result being reasonable since these samples are cooled slowly through T_g . When $T_q \geq T_g$, E_g becomes smaller to 2.40 eV, retaining the constant value in a region of $T_g \leq T_q \leq T_b$ (the boiling temperature⁴). It decreases further with T_q if $T_q \geq T_b$. The dependence of Γ on T_q is shown in Fig. 3(b). Al-

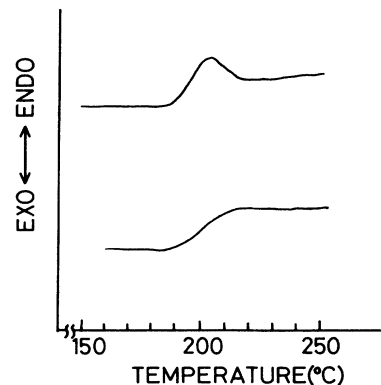


FIG. 1. DCS thermograms of slowly cooled (upper) and rapidly quenched (lower) samples from 950°C . Endo- and exothermic directions are indicated on the vertical axis.

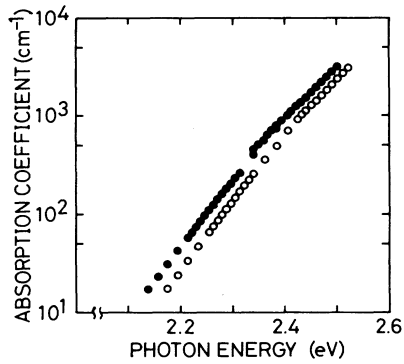


FIG. 2. Optical-absorption edges of slowly cooled (open circles) and rapidly quenched (solid circles) samples from 650°C.

though sample-to-sample variations of about ± 4 meV appear to be relatively large, it demonstrates that the quenched samples exhibit an abrupt change at T_g and an inflection at T_b .

Figure 3 includes the characteristics for the samples annealed at 180°C ($\approx T_g$). For the slowly cooled glasses and the samples quenched from temperatures of $T_q \leq T_g$, the annealing induces no appreciable changes. In contrast, upon the annealing all the samples quenched from

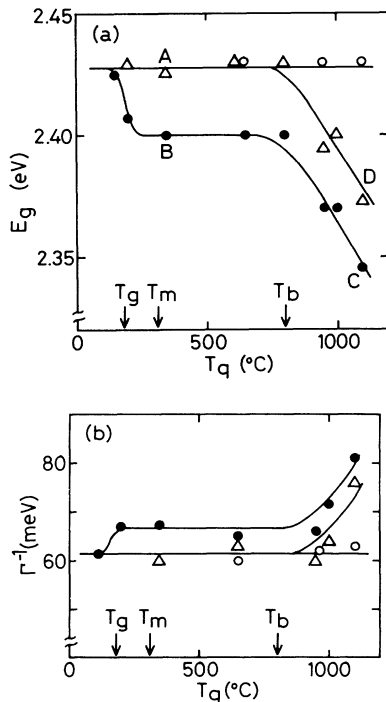


FIG. 3. The dependence of the energy gap E_g (a) and Γ^{-1} (b) on the temperature T_q , from which samples are slowly cooled (open circles) or quenched (solid circles). The results for samples, which have been quenched from T_q and then annealed at 180°C, are shown by triangles. The locations of T_g , T_m , and T_b are indicated by arrows. For A , B , C , and D in (a), see Fig. 5.

temperatures higher than T_g exhibit an increase in E_g of 30 meV, or a reduction of α by two factors, and a decrease in Γ^{-1} of ~ 5 meV. These changes may manifest approach to the stabilized state. It should be mentioned, however, that the glasses of $T_q \gtrsim T_b$ are, even after the annealing, different from the stabilized glass in respects of E_g and Γ^{-1} .

Figure 4 shows the correlation between E_g and Γ^{-1} , which is obtained by replotting the dependences on T_q depicted in Fig. 3. Also included in the figure are the results summarized by Street *et al.*¹² The results spreading at around $E_g = 2.4$ eV and $\Gamma^{-1} = 65$ meV are compatible with the present data, which indicate a negative correlation:

$$E_g \propto -\Gamma^{-1}. \quad (3)$$

It is worth mentioning in Fig. 4 that the results for as-prepared and annealed samples seem to be plotted on a common line. Cody *et al.*¹³ have discovered a similar proportionality for amorphous Si:H films having various H contents. Therefore, the relationship between E_g and Γ^{-1} appears to be universal to amorphous semiconductors. The correlation is predicted theoretically for generalized random structures.^{14,15} According to the argument given by Abe and Toyozawa,¹⁴ the relation is resulted from uncorrelated increases in interband potential fluctuations.

B. Raman scattering

In order to investigate the origin of the changes in the electronic properties, Raman scattering spectra of the samples denoted as A , B , C , and D in Fig. 3(a) were inspected. The results are shown in Fig. 5. Here, A represents the characteristics of the slowly cooled sample as well as the sample quenched from 350°C and then annealed at 180°C. Both of these may be regarded as reference materials in the following discussion.

The sample A shows two prominent peaks at ~ 350 cm^{-1} and ~ 30 cm^{-1} . The high-frequency peak is attributed to vibrational modes of pyramidal AsS_3 units.¹⁶ For the low-frequency Raman peak, interpretation of the origin has still been controversial.¹⁷⁻¹⁹

It is understood, however, that the peak contains information on medium-range structural correlations. Ac-

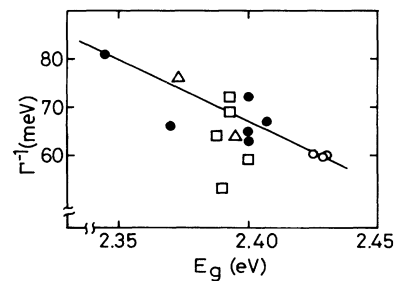


FIG. 4. The relationship between E_g and Γ^{-1} . Definition of the symbols is the same with that employed in Fig. 3, with addition of squares which indicate data summarized in Ref. 12.

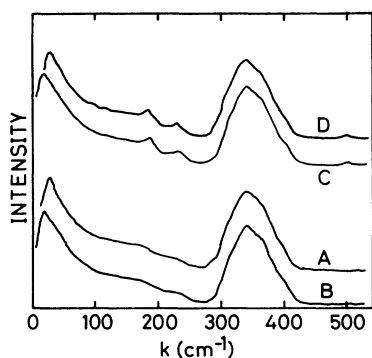


FIG. 5. Raman scattering spectra for samples *A*, *B*, *C*, and *D* defined in Fig. 3(a). k denotes the wave number.

cording to a recent study by Ahmad *et al.*,¹⁸ the Raman peak is ascribed to a non-Debye-type phonon density of states $g(\omega)$. They have demonstrated that $g(\omega)$ at around $\omega=0.5$ THz of quenched As_2S_3 samples is reduced by a heat treatment at 150°C , a stabilization process. This reduction accompanies a shift of the Raman peak to a higher wave number and a decrease in its intensity. The phonon mode of interest has a wavelength of $\sim 40 \text{ \AA}$, and therefore the reduction in the phonon density may imply decreases in structural fluctuations having similar spatial dimensions. In contrast, Strom and Freitas¹⁹ have argued on the basis of the distorted layer model²⁰ for the structure of glassy As_2S_3 that a higher-wave-number part in the low-frequency Raman peak can be attributed to the rigid-layer modes, which are observed in the layered As_2S_3 crystal. In light of their model, an increase in the medium-range order may provide an increase in the optic mode intensity, so that the low-frequency peak is seemingly shifted to higher frequencies. Thus both interpretations predict that when the medium-range structural correlation is enhanced, the peak frequency increases. We will, therefore, evaluate the degree of the medium-range structural order by k_{max} , the wave number of the low-frequency peak.

The difference between sample *A* and *B* lies in the low-frequency Raman peak, or in the medium-range correlations. The peak k_{max} of *B* is located in a lower wave number than that of *A*. This observation is understandable if the medium-range structure in *B* is more disordered than that in *A*. That is, the difference indicates that the annealing at T_g improves the medium-range order.

With regard to the Raman scattering spectra in Fig. 5, sample *C*, which is quenched from the higher temperature than T_b , shows two distinct features from the sample *A*. One is the position of the low-frequency peak, the consequence of which has been discussed in the above. In addition to this characteristic, we see small humps at around 230 cm^{-1} and 500 cm^{-1} in the spectrum for *C*. These peaks can be ascribed, respectively, to As—As and S—S homopolar bonds, on the basis of a compositional study for As-S glassy systems.²¹ It is

known that in glassy As-S systems heteropolar As—S bonds are energetically favored,¹¹ and accordingly the humps indicate inclusion of a small number of the homopolar bonds in the stoichiometric glass, i.e., a broken chemical order.

If we may assume that the intensity I_{230} of the Raman peak at 230 cm^{-1} is linearly dependent on the content of the As—As bond, the composition dependence of I_{230}/I_{350} , where I_{350} denotes the intensity of the As-S peak, implies that approximately 1% bonds are homopolar in sample *C*.⁴ This magnitude is comparable to the compositional uncertainty of the investigated samples, and whether the stoichiometry is retained in the sample or not might be doubtful. Nonetheless, we may speculate that the quenched sample contains appreciable numbers of the homopolar bonds with the reasons that the homopolar peaks were more conspicuous in all samples of $T_q \gtrsim T_b$ than in the stabilized sample [see Fig. 6(b)]. Moreover, the compositional uncertainty of 1% in x-ray microprobe analyses is attributable to the measuring process, and a real compositional variation is estimated to be smaller. We can, therefore, assert that sample *C* is stoichiometric, but it is degraded in respect of both medium-range and chemical orders.

Sample *D*, which is obtained through annealing *C*, exhibits the low-frequency peak similar to that in *A*. This means that the medium-range order is recovered by the

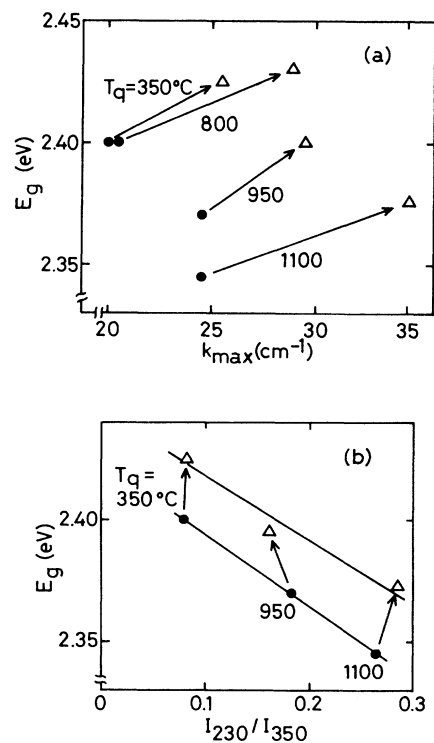


FIG. 6. The dependence of E_g on k_{max} (a) and on I_{230}/I_{350} (b) for samples having various T_q values. Results for as-quenched (circles) and annealed (triangles) glasses are shown, and changes induced by annealing at 180°C are depicted by arrows.

annealing. In contrast, however, no appreciable changes are induced in the homopolar bond peaks, suggesting that the annealing at 180°C is ineffective to convert the defective bonds to the heteropolar bonds.

C. Relations between electronic properties and structures

It is seen in Fig. 6(a) that in all samples investigated the annealing induces the increase in the structural order of $\Delta k_{\max} = 5 \sim 10 \text{ cm}^{-1}$ accompanying the increase in E_g of $\sim 30 \text{ meV}$. Therefore, we speculate a proportionality:

$$\Delta E_g^M \propto k_{\max} . \quad (4)$$

where ΔE_g^M expresses the change in E_g influenced from modifications in the medium-range order. Kawamura *et al.*¹⁷ have studied the dependence of energy gaps and Raman scattering spectra of As_2S_3 glasses on T_q , where $170^\circ\text{C} \leq T_q \leq 400^\circ\text{C}$ in their work. Their results exhibit a tendency similar to that shown in Fig. 6(a).

Taking the Raman scattering results into account, we can connect the further decrease in E_g of the quenched sample *C* from that in *B* to the broken chemical order. A possibility that the homopolar bonds in a stoichiometric glass, or “wrong” bonds, produce electronic defect states at band edges which lessen the energy gap has been theoretically predicted by Vanderbilt and Joannopoulos.²² It is also demonstrated experimentally that deposited GeS_2 films containing a large number of homopolar bonds exhibit the optical-absorption edges located at lower energies than that of bulk GeS_2 glasses.³

Figure 6(b) shows the relation between E_g and the normalized intensity of the Raman peak attributable to As—As bonds. Within the experimental errors of $\pm 0.01 \text{ eV}$ for E_g and ± 0.01 for the intensity, each results for as-quenched and annealed states seem to be plotted on straight lines representing negative proportionalities,

$$\Delta E_g^C \propto -I_{230} , \quad (5)$$

where ΔE_g^C denotes the change in E_g induced with the chemical disorder. In this figure the effect of the annealing is represented approximately as shifts along the vertical direction. That is, no changes in the homopolar density are induced with the annealing. The fact that only the medium-range order is recovered with annealing at T_g [Fig. 6(a)] while the covalent bonds are intact is compatible with a model proposed for structural relaxation at T_g .²³

The dependence of E_g on the homopolar-bond density gives insight to electronic states at the band edges. As was mentioned in the previous section, the homopolar-bond density of the quenched sample of $T_q = 1100^\circ\text{C}$ is estimated to be 1 at.%. This means, under an assumption of a homogeneous distribution of the defective bonds, that the separation between them is $\sim 10 \text{ \AA}$, since the atomic volume of As_2S_3 glass is $\sim 15 \text{ \AA}^3/\text{atom}$. In contrast, Fig. 6(b) suggests that the defect density in the stabilized sample is approximately one third of the quenched glass, which can be converted to the separation of $\sim 20 \text{ \AA}$. Accordingly, we may assume that the

reduction in the distance between the defects from $\sim 20 \text{ \AA}$ to $\sim 10 \text{ \AA}$ is responsible for the shrinkage in E_g of $\sim 30 \text{ meV}$.

As shown in Fig. 6, two kinds of disorders affect additively on E_g , and thus we can summarize the above argument as

$$E_g = 2.43 \text{ (eV)} - \Delta E_g^M - \Delta E_g^C . \quad (6)$$

where 2.43 eV is the energy gap of the stabilized glass. The second term expresses the effect of potential fluctuations relating to the medium-range structure, and the third term is ascribed to fluctuations arising from the wrong bonds.

The change in the Urbach parameter shown in Fig. 4 is consistent with the present model assuming the structural modifications. It is accepted that the parameter Γ reflects the degree of structural randomness, although a theoretical understanding on the origin of the Urbach tail is still in infancy.¹¹ It becomes smaller with increasing disorder. Thus the observations that the quenched samples have smaller Γ can be attributed to the increase in the structural randomness, which reduces E_g as was discussed in the above. By recalling Eq. (3), we may obtain an expression for Γ^{-1} similar to that for E_g in Eq. (6).

In order to examine further the annealing effects on E_g , the quenched samples from 1000°C were heat treated at various temperatures. As shown in Fig. 7, the sample annealed at $T_a \geq T_g$ shows an increase in E_g , which has been ascribed to the recovering of the medium-range order. In a higher T_a region, the scattering of data becomes greater with presently unknown reasons. Nonetheless, it seems that a further increase in E_g occurs when $T_a \geq 600 \text{ K} \simeq T_m$ (the melting temperature), and upon the annealing the quenched glasses show a similar E_g to that of the stabilized glass.

This result appears to be irrational, since in a glassy material the melting temperature has no physical consequences. The change between liquid and super-cooled states is continuous and smooth for good glass formers, and indeed DSC studies could detect no specific signals at around 600 K. It is also worthwhile to mention that T_g of As-S glassy systems is lower than 470 K,²³ which deviates significantly from the temperature of interest.

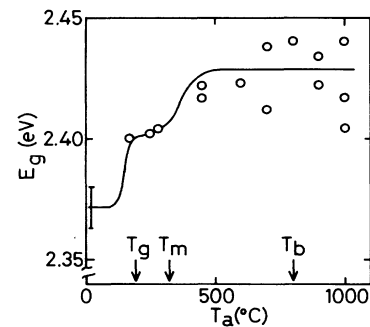


FIG. 7. The dependence of the energy gap E_g of samples quenched from 1000°C on the annealing temperature T_a .

The mechanism for which the annealing at $T_a \gtrsim T_m$ is effective to stabilize the quenched glasses is not understood at present.

Correlation between the magnitude of the optical bandgap and structures in evaporated As_2S_3 is discussed here. It is known that² as-evaporated As_2S_3 films have comparable energy gaps with that of the stabilized glass. In addition, Nemanich and Street *et al.*²¹ have demonstrated through Raman scattering and EXAFS studies that the as-evaporated films are constructed with many small molecules containing homopolar bonds. The existence of the wrong bonds contributes to a decrease in energy gaps as expressed by Eq. (6). However, electron wave functions may be strongly localized in the molecules, and lessen bandwidths as demonstrated by ultraviolet photoemission spectroscopy (UPS) studies.²⁴ This molecular effect may cancel the chemical influence, resulting in the similar optical-absorption edge.

There seems to exist some connections between the quenched As_2S_3 glass and annealed films in respect of amorphous structures. Historically, it had been assumed that there are no gross structural differences between the films which were annealed at T_g and bulk glasses.² Hamanaka *et al.*, however, have discovered that the optical-absorption edge of annealed films is located in a lower-energy side than that of annealed bulk samples.²⁵ Furthermore, Nemanich *et al.* have shown that annealing cannot induce complete transformations from homopolar to heteropolar bonds.²¹ Kosek *et al.* have demonstrated the existence of the defective bonds in films by using a novel chemical technique.²⁶ It is, therefore, envisaged that the structure of the annealed films resembles that of the bulk glasses which are quenched from $T_q > T_b$ and then annealed at T_g . Most of bulk glasses prepared in previous studies are quenched from temperatures of $T_q < T_b$, so that these may contain a smaller number of homopolar bonds.

It may be worthwhile to mention that the structure of quenched glasses of $T_q \gtrsim T_b$ is distinct from that of as-deposited films mainly consisting of spherical molecules.^{2,21} This may suggest that, although both materials are prepared through vapour phase, the quenching in bell jars is much milder than that in small ampoules.

IV. SUMMARY

Dependence of atomic and electronic structures of glassy As_2S_3 on preparation methods and annealing treatments has been studied. The amorphous structure

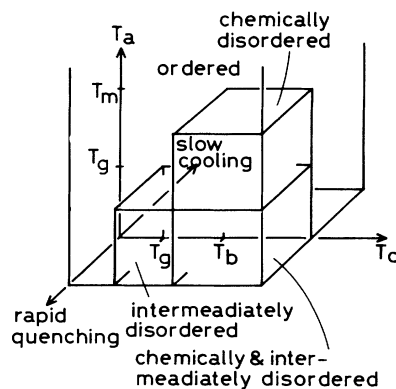


FIG. 8. The dependence of chemical and medium-range orders on the quenching temperature T_q , the annealing temperature T_a , and the quenching rate.

is modified by changes in three parameters, i.e., the temperature from which the melt is quenched, the quenching rate, and the annealing temperature. The present result can be summarized as shown in Fig. 8. Slowly cooled samples are mostly stabilized. Samples quenched into water from temperatures between T_g and T_b are lacking mainly in medium-range orders. Samples quenched from higher temperatures are in addition chemically disordered. To improve the medium-range order, annealing at temperatures above T_g is required, whereas the chemical order is recovered with annealing above T_m .

It has also been discovered that the optical-absorption edge is affected with the two kinds of structural disorders. Accompanying the increase in the disorders, the optical absorption edge is red shifted with decreasing its slope. The influence of the disorders on the position and the steepness parameters of the Urbach tail are represented by the additional formula. Characteristics of deposited As_2S_3 can be understood as influenced by the chemical disorder and molecularity.

ACKNOWLEDGMENTS

The author would like to thank Professor S. Minomura and Professor J. Nakahara for use of Raman scattering equipment, and to Mrs. M. Tazawa and R. Kawase for their experimental assistance. The present work is partially supported by The Asahi Glass Foundation for Industrial Technology.

¹A. E. Owen, in *Electronic and Structural Properties of Amorphous Semiconductors*, edited by P. G. LeComber and J. Mort (Academic, London, 1973), p. 161.

²J. P. DeNeufville, in *Optical Properties of Solids-New Developments*, edited by B. O. Seraphin (North-Holland, Amsterdam, 1975), p. 437.

³L. Tichy, A. Triska, H. Ticha, and M. Frumar, *Philos. Mag. B*

54, 219 (1986); K. Tanaka, Y. Kasanuki, and A. Odajima, *Thin Solid Films* **117**, 251 (1984).

⁴K. Tanaka, S. Gohda, and A. Odajima, *Solid State Commun.* **56**, 899 (1985).

⁵K. Tanaka and A. Odajima, *J. Non-Cryst. Solids* **46**, 259 (1981).

⁶W. S. Rodney, I. H. Malitson, and T. A. King, *J. Opt. Soc.*

- Am. **48**, 633 (1958).
- ⁷K. Tanaka and Y. Ohtsuka, *J. Appl. Phys.* **49**, 6132 (1978).
- ⁸Z. Cimpl, F. Kosek, V. Husa, and J. Svoboda, *Czech. J. Phys. B* **31**, 1191 (1981).
- ⁹D. G. Semak, V. I. Mikla, I. P. Mikhal'ko, V. A. Stefanovich, V. Yu. Slivka, and Yu. M. Vysochanskii, *Fiz. Tverd. Tela (Leningrad)* **26**, 3210 (1984) [*Sov. Phys. Solid State* **26**, 1934 (1984)].
- ¹⁰K. Tanaka, *Shinku* **28**, 615 (1985) (in Japanese).
- ¹¹N. F. Mott and E. A. Davis, *Electronic Processes in Non-Crystalline Materials* (Clarendon, Oxford, 1979).
- ¹²R. A. Street, T. M. Searle, I. G. Austin, and R. S. Sussmann, *J. Phys. C* **7**, 1582 (1974).
- ¹³G. D. Cody, T. Tiedje, B. Abeles, B. Brooks, and Y. Goldstein, *Phys. Rev. Lett.* **47**, 1480 (1981).
- ¹⁴S. Abe and Y. Toyozawa, *J. Phys. Soc. Jpn.* **50**, 2185 (1981).
- ¹⁵J. Szczyrbowski, *Phys. Status Solidi B* **113**, 715 (1982).
- ¹⁶S. Itoh and T. Fujiwara, *J. Non-Cryst. Solids* **51**, 175 (1982); R. J. Kobliska and S. A. Solin, *Phys. Rev. B* **8**, 756 (1973).
- ¹⁷H. Kawamura, T. Takasuka, T. Minato, T. Hyodo, and T. Okumura, *J. Non-Cryst. Solids* **59&60**, 863 (1983).
- ¹⁸N. Ahmad, K. W. Hutt, and W. A. Phillips, *J. Phys. C* **19**, 3765 (1986).
- ¹⁹U. Strom and J. A. Freitas, Jr., *Solid State Commun.* **59**, 565 (1986).
- ²⁰R. Zallen, *The Physics of Amorphous Solids* (Wiley, New York, 1983), p. 86.
- ²¹R. J. Nemanich, G. A. N. Connell, T. M. Hayes, and R. A. Street, *Phys. Rev. B* **18**, 6900 (1978); R. A. Street, R. J. Nemanich, and G. A. N. Connell, *ibid.* **B 18**, 6915 (1978).
- ²²D. Vanderbilt and J. D. Joannopoulos, *Phys. Rev. B* **23**, 2596 (1981).
- ²³K. Tanaka, *Solid State Commun.* **54**, 867 (1985).
- ²⁴T. Takahashi and Y. Harada, *Solid State Commun.* **35**, 191 (1980).
- ²⁵H. Hamanaka, K. Tanaka, and S. Iijima, *Solid State Commun.* **23**, 63 (1977).
- ²⁶F. Kosek, Z. Cimpl, J. Tulka, and J. Chlebny, *J. Non-Cryst. Solids* **90**, 401 (1987).